

Utilizing entropy to systematically quantify the resting-condition baroreflex regulation function

Bo-Yuan Li,^{1,2} Xiao-Yang Li,^{1,2,*} Xia Lu,^{3,*} Rui Kang,^{1,2} Zhao-Xing Tian,⁴ Feng Ling³

¹ School of Reliability and Systems Engineering, Beihang University, Beijing 100191, China

² Science and Technology on Reliability and Environmental Engineering Laboratory, Beijing 100191, China

³ Department of Neurosurgery, Xuanwu Hospital, Capital Medical University and China International Institution of Neuroscience, Beijing 100053, China

⁴ Department of Emergency, Beijing Jishuitan Hospital, Beijing 100035, China

*Correspondence: Xiao-Yang Li, leexy@buaa.edu.cn; Xia Lu, luxia@xwhosp.org

Abstract

Baroreflex is critical to maintain the blood pressure homeostasis, and the quantification of the baroreflex regulation function (BRF) can provide guidance for disease diagnosis, treatment and healthcare. Current quantification of the BRF such as baroreflex sensitivity cannot represent the BRF systematically. From the perspective of complex systems, we regard that the BRF is the emergence result of the diverse states and interactions in the physiological mechanisms. Therefore, the three-layer emergence is constructed in this work, which is from the physiological mechanisms to the physiological indexes and then to the BRF. On this basis, since the entropy in statistical physics macroscopically measures the diversity of the system's states, a new index called the PhysioEnt is proposed to represent the BRF and quantify the physical relationships between the BRF and four physiological indexes, baroreflex sensitivity, heart rate, heart rate variability, and systolic blood pressure. Based on the proposed method, some new findings with medical significance are obtained, including the mechanisms that aging and obesity affect the resting-condition BRF are different, and the resting-condition BRFs of men and older people depend more on the physiological processes among organs/tissues. Based on the measurable indexes, the proposed method would support the individualized medicine prospectively.

1. Introduction

The arterial baroreceptor reflex (referred to baroreflex) is one of the mechanisms for maintaining the blood pressure homeostasis, and the baroreflex function, i.e. BRF, is to restore the deviated blood pressure to optimal level in short time. The weakening or failure of BRF plays an important role in various diseases: not only the chronic diseases such as hypertension, postural hypotension, and paroxysmal syncope [1], but also some acute lethal conditions such as stroke [2] and myocardial infarction [3]. If we can figure out some quantitative indexes to represent the intensity of BRF and model the relationships between the BRF and some measurable physiological indexes related to baroreflex, especially including blood pressure, heart rate, heart rate variability, and baroreflex sensitivity, we can provide support for the individual diagnosis, treatment, and health management of related diseases.

To quantify the BRF, some researches focused on the typical physiological indexes and construct the relation curves between these indexes based on experiments. Such relation curves include the curves of baroreflex sensitivity with peripheral osmolality [4] and blood volume [5], and the curves of blood pressure with carotid sinus pressure [6], R-R interval [7] and nerve activity [8, 9]. However, these physiological indexes cannot systematically characterize the BRF actually. For instance, the typical quantification of the BRF, baroreflex sensitivity, has been proved that it mainly reflect the function of the efferent nerves but not the afferent pathway [10, 11]. In addition, the relation curves obtained by experiments cannot clearly correspond to specific physiological mechanisms, which limits the appliances in the disease diagnosis and treatment.

Some researches adopted differential equations and automatic control models to quantify the BRF based on the physiological mechanisms, such as the modeling of the cardiovascular and autonomic nervous system [12-16], and coupling modeling with other physiological systems [17-19]. However, such researches still have some problems: due to the complexity of human physiological mechanisms, the accurate modeling requires a large amount of detailed data and information which are difficult to obtain limited by experimental conditions. Specifically, when determining the parameters of a control element, the measurements in the open-loop case are necessary to exclude the influences of other control elements. For this purpose, the normal regulation would be blocked, and certain organs would be isolated out [20]. However, such experiments are forbidden for human ethically. Many researches applied the results from animal experiments instead [21, 22], but the applicability of these results to human is quite doubtful.

Some researches utilized the information-based methods [23-26] to analyze the information flows and causal relationships among the physiological indexes, including blood pressure, pulse interval, and sympathetic nervous activity. In addition, the concept of the physiological network was proposed to model the interactions among various indexes [27]. These researches constructed the interactions among the measurable indexes, which provided concise descriptions of the complex physiological mechanisms. However, these researches still lacked a systematic representation of the BRF over the interactions among indexes.

From the above literature review, it can be realized that we still lack a quantitative relationship between a systematic index of the BRF and measurable physiological indexes. Actually, some medical researches have identified the relationships between the diversity of measurable physiological indexes and the resting-condition baroreflex. Cloarec [28] and Nikolaou [29] reported that there are spontaneous fluctuations of the indexes related to the resting-condition baroreflex without external perturbations. The studies from Meyer [30] and He [31] showed that, for healthy individuals, the physiological indexes usually remain in relatively stable fluctuating states, neither chaotic and disordered, nor unchangeable. In contrast, many pathological conditions are accompanied by an alteration or disappearance of typical fluctuations [32]. Furthermore, the fluctuations of physiological indexes originate from the intrinsic regulation mechanisms [33, 34]. Chiesa [35] and Hu [36] also pointed out that the fluctuating states reflect the complicated coupling of the components in the baroreflex-related regulation. In other words, the regulation function emerges from these states and interactions [37].

The above physiological findings and statistical physics inspire our thinking: we can systematically quantify BRF directly based on the physiological mechanisms and the easily measured data of physiological indexes in clinic and daily life by using the method of entropy. In statistical physics, entropy is a systematical characterization of the microscopic diversity, and it has been successfully adopted to describe the complex systems such as robot groups [38], urban development [39], and proteins [40]. Therefore, it is sound to utilize the entropy to construct the connection between the BRF and physiological mechanisms.

In this work, we focus on the resting-condition BRF and construct the emergence from the baroreflex mechanisms to the physiological indexes and then to the BRF quantified by the entropy. Specifically, four indexes, baroreflex sensitivity, systolic blood pressure, heart rate, and heart rate variability, can represent different mechanisms respectively. Based on the four indexes, a maximum entropy model is constructed to calculate the entropy and characterize the resting-condition BRF. We then propose a relative contribution index to study and compare the effects of specific physiological processes and organs/tissues on the resting-condition BRF. The monitoring data of more than 1000 individuals from Jena University Hospital is utilized to establish the model and conduct analysis. And the medical findings can support the diagnosis, treatment, and healthcare of related diseases. Furthermore, since the proposed methods in this work are based on measurable physiological indexes, they can be adopted briefly in daily life with the appliance of wearable devices, and support the individualized healthcare.

2. The emergence in the resting-condition BRF

Baroreflex is a typical feedback regulation, and the physiological mechanisms of the baroreflex can be concluded as: when blood pressure fluctuates, the blood vessels stretch, and the baroreceptors are stimulated. The nerve impulses are integrated in the nerve centers and affect the sympathetic and parasympathetic activities. Then the sinus nodes and other effectors are innervated to achieve the short-term regulation of blood pressure. For the resting condition, it can be assumed that the sympathetic activity is essentially unchanged and has little effect on the regulation of blood pressure [11].

To represent the above complicated physiological mechanisms, some physiological indexes are proposed. Physiological indexes represent whether the organs/tissues in the baroreflex achieve their functions, and also reflect whether the physiological processes among the organs/tissues are normal.

Among various indexes, baroreflex sensitivity (BRS) is the typical index to measure the behavior of the baroreflex. However, essentially, BRS describes the reflex effect of the sinus nodes in response to the nerve impulses, but cannot accurately reflect how the nerve impulses generate [41]. In other words, BRS mainly represents the function of the efferent parasympathetic nerves, and reflects the process that the parasympathetic nerves innervate the sinus nodes and regulate blood pressure. But BRS cannot reflect the process in the afferent pathway [10].

For this point, heart rate variability (HRV) is calculated and studied. Studies showed that HRV can effectively quantify the nerve impulses in the afferent pathway, especially the parasympathetic activities [42, 43]. Therefore, HRV represents the function of the afferent parasympathetic nerves, and reflects the process that the baroreceptors generate impulses and stimulate the parasympathetic nerves [44].

In addition to the functions of the nerves in the baroreflex, the functions of the effectors, i.e. the sinus nodes and the blood vessels, should be considered. The function of the sinus nodes is to generate electrical impulses and cause the heartbeats. Therefore, heart rate (HR) is the index that directly represents the function of the sinus nodes. In the baroreflex, the blood vessels are pressed, and the baroreceptors are stimulated. Systolic blood pressure (SBP) directly indicates how much the artery walls are exerted by the blood, and has significant relationships with the vascular elasticity and the stretching of vessel walls [45, 46]. Therefore, SBP is utilized to represent the function of the blood vessels in this work.

According to the above analysis, the four measurable physiological indexes, BRS, HRV, HR, and SBP can cover the main organs/tissues and physiological processes in the resting-condition baroreflex. Neither of them, including BRS, can comprehensively represent the regulation function alone, but the synergy and interaction among these indexes can emerge the

resting-condition BRF. Therefore, the emergence process from the physiological mechanisms to the physiological indexes and then to the BRF can be constructed. Specifically, the baroreflex physiological mechanisms are in the bottom layer, which contain the specific organs/tissues and physiological processes. The physiological indexes BRS, SBP, HR, and HRV belong to the middle layer, and the interactions among the indexes should be considered due to the coupling of the mechanisms. Finally, the resting-condition BRF is in the top layer. Such an emergence process is conceptualized in Figure 1.

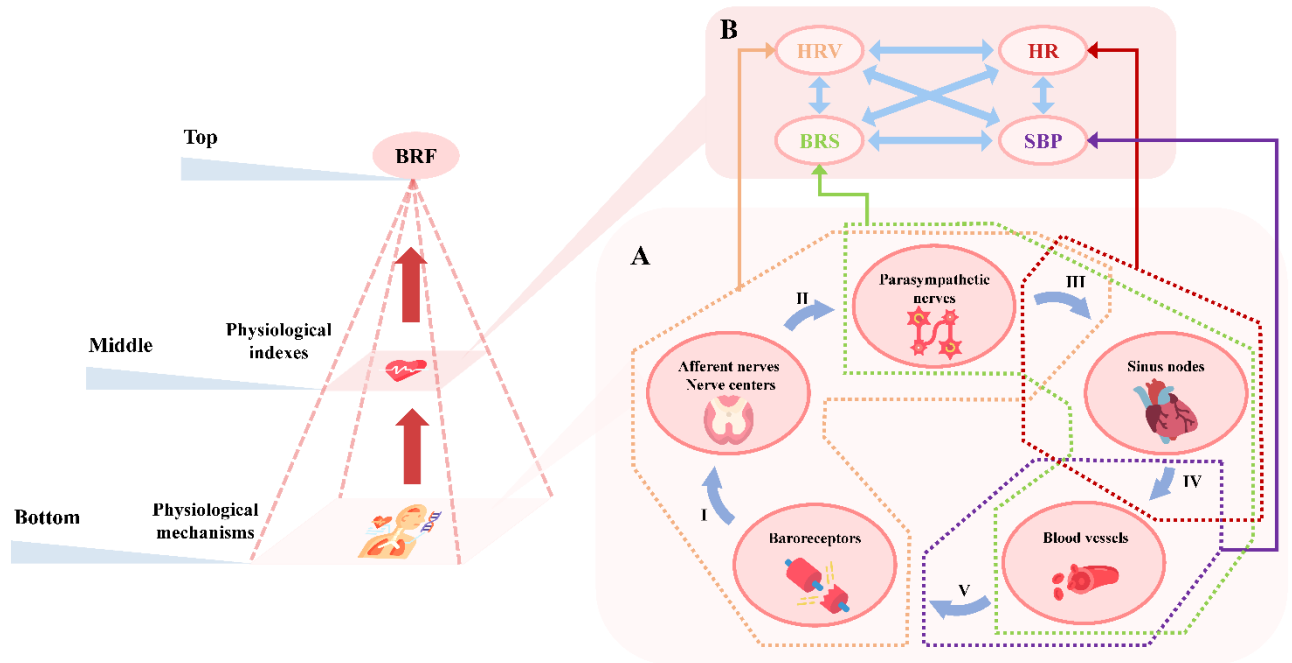


Figure 1. Emergence from the physiological mechanisms to the physiological indexes and the BRF. (A): For the physiological mechanisms, the nodes indicate the organs/tissues, and the arrows indicate the physiological processes, where: I) Impulses generated by the baroreceptors transmit through the afferent pathway and integrate in the nerve centers; II) The nerve centers innervate the parasympathetic activities; III) The parasympathetic nerves innervate the sinus nodes to change heart rate; IV) Heart rate influences blood pressure and the stretching of the blood vessels; V) The baroreceptors sense the stretching. The dashed parts indicate the emerged indexes corresponding to different organs/tissues and processes. (B): The physiological indexes, BRS, SBP, HR, and HRV, emerge from the physiological mechanisms. The arrows indicate the possible interactions among the indexes.

According to the review in section 1, it is reasonable to regard that the fluctuations of BRS's, SBP's, HR's and HRV's states characterize the resting-condition BRF. If we can quantify the fluctuations of the four indexes, we can quantitatively evaluate the resting-condition BRF based on these indexes.

3. Methods

3.1. The physiological entropy and the maximum entropy model

Entropy is the foundation of statistical physics and measures the diversity of a thermodynamic system. Shannon developed the entropy in information theory, which measures the diversity inherent to the states of systems. The entropy of a discrete random variable X was proposed first, and then the concept of entropy was extended by Shannon to the continuous condition, as shown in Eq. 1:

$$H(X) = \begin{cases} -\sum_{i=1}^n P(x_i) \ln P(x_i), & \text{if } X \text{ is discrete-valued} \\ -\int P(x) \ln P(x), & \text{if } X \text{ is continuous-valued} \end{cases} \quad (1)$$

where: $H(X)$ is the entropy of X and P is the probability of X .

Further, Jaynes figured out that statistical physics is only to do probabilistic inferences from limited information and, therefore, combined the entropy in statistical physics and information theory [47, 48]. In a word, entropy macroscopically measures how a system's microscopic diversity emerges the system's behaviors and the capacities of the system's functions. Therefore, it can quantify the fluctuating states of the four physiological indexes; consequently, construct the connection between the BRF and physiological mechanisms.

The states of the four physiological indexes, i.e., BRS, SBP, HR, and HRV, form a four-dimensional continuous-valued vector. However, when calculating the entropy of the continuous-valued vector, the continuous entropy in Eq. 1 has been proved to be problematic [49]. Therefore, in this work, the continuous indexes are normalized and partitioned into fixed value spaces for discretization, which is further introduced in section 3.3. Through the data preprocessing, the four-dimensional vector composed of the discrete random variables representing the physiological indexes, $\mathbf{x} = \{x_{\text{BRS}}, x_{\text{SBP}}, x_{\text{HR}}, x_{\text{HRV}}\}$, can be obtained. And the physiological entropy S , PhysioEnt for short, can be defined as:

$$S = -\sum_{\mathbf{x}} P(\mathbf{x}) \ln P(\mathbf{x}) \quad (2)$$

According to Eq. 2, the more diverse the states of physiological indexes are, the more significant the fluctuations are; and then the larger the PhysioEnt is; otherwise, the smaller PhysioEnt corresponds to the less significant fluctuations. Since it is reported [30, 31] that the fluctuations of physiological indexes in healthy individuals are in a relatively stable range, the PhysioEnt is also supposed to be within a stable range for healthy individuals. In other words, the PhysioEnt is a kind of performance index to evaluate the resting-condition BRF. If the PhysioEnt of an individual from some population exceeds the limits of this population's stable range, it suggests that this individual may be in some unhealthy state.

Further, when calculating the PhysioEnt, it is expected to be based on the physical model that can reflect the physiological mechanisms rather than the phenomenological statistical estimates. Therefore, the principle of maximum entropy is adopted, and the maximum entropy model of the $P(\mathbf{x})$ in Eq. 2 is constructed. The principle of maximum entropy indicates that the probability distribution with the largest entropy is the best choice to represent the current knowledge about a system [47, 48], which provides brief and conservative solutions for systems. The maximum entropy model is the model which can judge and quantify the interactions among the factors in a system, and has been generally utilized in biology and medical fields, such as the gene regulation [50] and the brain connectivity [51]. Specifically, in the maximum entropy model, the interactions among factors are represented by the model components composed of these factors. In this work, to calculate the PhysioEnt and reflect the physiological mechanisms, the basic form of the maximum entropy model of $P(\mathbf{x})$ can be written as:

$$P(\mathbf{x}) = \frac{1}{Z} \exp \left[\sum_{\mu=1}^N \lambda^{\mu} f^{\mu}(\mathbf{x}) \right] \quad (3)$$

where Z is a parameter for normalization, $f^{\mu}(\mathbf{x})$ means the μ^{th} model component, λ^{μ} is the model parameter corresponding to $f^{\mu}(\mathbf{x})$ and N is the total number of components.

Different model components represent different inter-dependencies among the indexes, and will lead to different maximum entropy models. Besides the independent effects reflected by x_{BRS} , x_{SBP} , x_{HR} and x_{HRV} , the interactions between two indexes can be represented by the model components obtained by multiplying two indexes, i.e. $x_{\text{BRS}}x_{\text{SBP}}$. Similarly, the interactions among three indexes and four indexes can also be represented by model components such as $x_{\text{BRS}}x_{\text{SBP}}x_{\text{HR}}$ and $x_{\text{BRS}}x_{\text{SBP}}x_{\text{HR}}x_{\text{HRV}}$. The models considering the interactions between two indexes, among three indexes and among four indexes are respectively called Pairwise model $P_{\text{II}}(\mathbf{x})$, Triplet model $P_{\text{III}}(\mathbf{x})$ and Quaternion model $P_{\text{IV}}(\mathbf{x})$. For example, the specific form of $P_{\text{II}}(\mathbf{x})$ is:

$$\begin{aligned}
P_{\text{II}}(\mathbf{x}) &= \frac{1}{Z_{\text{II}}} \exp \left[\sum_{\mu=1}^{10} \lambda_{\text{II}}^{\mu} f_{\text{II}}^{\mu}(\mathbf{x}) \right] \\
&= \frac{1}{Z_{\text{II}}} \exp \left[\lambda_{\text{II}}^1 x_{\text{BRS}} x_{\text{SBP}} + \lambda_{\text{II}}^2 x_{\text{BRS}} x_{\text{HR}} + \lambda_{\text{II}}^3 x_{\text{BRS}} x_{\text{HRV}} + \lambda_{\text{II}}^4 x_{\text{SBP}} x_{\text{HR}} \right. \\
&\quad \left. + \lambda_{\text{II}}^5 x_{\text{SBP}} x_{\text{HRV}} + \lambda_{\text{II}}^6 x_{\text{HR}} x_{\text{HRV}} + \lambda_{\text{II}}^7 x_{\text{BRS}} + \lambda_{\text{II}}^8 x_{\text{SBP}} + \lambda_{\text{II}}^9 x_{\text{HR}} + \lambda_{\text{II}}^{10} x_{\text{HRV}} \right], Z_{\text{II}} \\
&= \sum_{\mathbf{x}} \exp \left[\sum_{\mu=1}^{10} \lambda_{\text{II}}^{\mu} f_{\text{II}}^{\mu}(\mathbf{x}) \right]
\end{aligned} \tag{4}$$

For the solutions of the model parameters, λ_k^{μ} , $k = \text{II}, \text{III}, \text{IV}$, we adopt the iterative scaling algorithm [52]:

$$(\lambda_k^{\mu})_{t+1} = (\lambda_k^{\mu})_t + \alpha \times \text{sign}(\langle f_k^{\mu}(\mathbf{x}) \rangle_D) \times \ln \left(\frac{\langle f_k^{\mu}(\mathbf{x}) \rangle_D}{\langle f_k^{\mu}(\mathbf{x}) \rangle_t} \right) \tag{5}$$

where: $(\lambda_k^{\mu})_t$ is the λ_k^{μ} after the t^{th} iteration; $\langle f_k^{\mu}(\mathbf{x}) \rangle_D$ is the expectation of $f_k^{\mu}(\mathbf{x})$ calculated by data, $\langle f_k^{\mu}(\mathbf{x}) \rangle_t$ is the expectation of $f_k^{\mu}(\mathbf{x})$ in the model after the t^{th} iteration, α is the learning rate that is set as 0.75 and $\text{sign}(\cdot)$ is the signum function which is defined as $\text{sign}(x) = \begin{cases} -1 & \text{if } x < 0, \\ 0 & \text{if } x = 0, \\ 1 & \text{if } x > 0. \end{cases}$. The stop condition of the iteration is that: $\sum_{\mu=1}^{N_k} \left\{ \frac{|\langle f_k^{\mu}(\mathbf{x}) \rangle_D - \langle f_k^{\mu}(\mathbf{x}) \rangle_t|}{\langle f_k^{\mu}(\mathbf{x}) \rangle_D} \times 100\% \right\} \leq 0.5\%$, where N_k is the total number of the model components. $\langle f_k^{\mu}(\mathbf{x}) \rangle_t$ is calculated by the Metropolis-Hasting algorithm.

The rationalities of $P_{\text{II}}(\mathbf{x})$, $P_{\text{III}}(\mathbf{x})$, and $P_{\text{IV}}(\mathbf{x})$ can be computed based on the multi-information ratio, η_k [53] to support the model selection:

$$\eta_k = \frac{S_{\text{ind}} - S_k}{S_{\text{ind}} - S_D}, k = \text{II}, \text{III}, \text{IV} \tag{6}$$

where: S_{ind} is the PhysioEnt of $P_{\text{ind}}(\mathbf{x})$. $P_{\text{ind}}(\mathbf{x})$ is the distribution considering no interaction, that is, $P_{\text{ind}}(\mathbf{x}) = P(x_{\text{BRS}}) \times P(x_{\text{SBP}}) \times P(x_{\text{HR}}) \times P(x_{\text{HRV}})$, and $P(x_{\text{BRS}})$, $P(x_{\text{SBP}})$, $P(x_{\text{HR}})$ and $P(x_{\text{HRV}})$ are the marginal distributions of the corresponding indexes; S_k is the PhysioEnt of $P_k(\mathbf{x})$ and S_D is the PhysioEnt of the observed data. η_k measures the similarity between $P_k(\mathbf{x})$ and data in terms of information gain. The closer to 1 the η_k is, the more reliable $P_k(\mathbf{x})$ is.

3.2. The relative contributions of the model components

From the perspective of the model itself, it is composed of various model components. Take $P_{\text{II}}(\mathbf{x})$ as an example: the model components in $P_{\text{II}}(\mathbf{x})$ can be divided into interactive components including $x_{\text{BRS}}x_{\text{SBP}}$, $x_{\text{BRS}}x_{\text{HR}}$, $x_{\text{BRS}}x_{\text{HRV}}$, $x_{\text{SBP}}x_{\text{HR}}$, $x_{\text{SBP}}x_{\text{HRV}}$ and $x_{\text{HR}}x_{\text{HRV}}$, and independent components including x_{BRS} , x_{SBP} , x_{HR} and x_{HRV} .

From Figure 1, we can figure out that these independent components correspond to the elements in the physiological indexes layer. And these interactive components correspond to the interactions between every two elements in this layer. Further, we can regard the interactive components as specific physiological processes in the physiological mechanisms layer (see Supplementary Texts in Supplementary materials for details), and regard the independent components as specific organs/tissues (see section 2 for details). Therefore, if we can figure out how much each component contributes to $P_{II}(\mathbf{x})$, the corresponding results can indicate how and how much the associated physiological processes or organs/tissues make effects on the resting-condition BRF.

To quantify the contribution of each model component, we propose the concept of relative contribution and its quantitative index RC . First, we define the concept of generalized energy, $E(\mathbf{x})$, as shown in Eq. 7, where $f_{II}^{\mu}(\mathbf{x})$ represents the μ^{th} model component and λ_{II}^{μ} is the corresponding parameter. According to Eq. 4, $E(\mathbf{x})$ is the numerator of $P_{II}(\mathbf{x})$, and the total number of model components of $P_{II}(\mathbf{x})$ is 10.

$$E(\mathbf{x}) = \exp \left[\sum_{\mu=1}^{10} \lambda_{II}^{\mu} f_{II}^{\mu}(\mathbf{x}) \right] = \prod_{\mu=1}^{10} \exp[\lambda_{II}^{\mu} f_{II}^{\mu}(\mathbf{x})] \quad (7)$$

Since the denominator of $P_{II}(\mathbf{x})$ is a parameter for normalization, the value of $E(\mathbf{x})$ determines the value of $P_{II}(\mathbf{x})$, and then determines the value of the PhysioEnt according to Eq. 2. The greater the $E(\mathbf{x})$ is, the greater the $P_{II}(\mathbf{x})$ is, and the greater possibility that the values of indexes are \mathbf{x} is.

Then, the energy proportion of the v^{th} model component given \mathbf{x} , $R_v(\mathbf{x})$, is defined. $R_v(\mathbf{x})$ represents the portion of $E(\mathbf{x})$ occupied by the v^{th} model component given \mathbf{x} . Since $E(\mathbf{x})$ is calculated by multiplying the exponential functions of all model components, $R_v(\mathbf{x})$ can be expressed as:

$$R_v(\mathbf{x}) = \frac{\exp[\lambda_{II}^v f_{II}^v(\mathbf{x})]}{E(\mathbf{x})} = \frac{1}{\prod_{\mu \neq v} \exp[\lambda_{II}^{\mu} f_{II}^{\mu}(\mathbf{x})]} \quad (8)$$

The greater the $R_v(\mathbf{x})$ is, the more significantly $E(\mathbf{x})$ depends on the v^{th} model component. Therefore, it can be inferred that the v^{th} model component contributes more significantly to $P_{II}(\mathbf{x})$ and the PhysioEnt. Based on $R_v(\mathbf{x})$, RC_v is defined as the result after normalizing for all model components and averaging for all \mathbf{x} , as shown in Eq. 9. Essentially, RC_v reflects the contribution of the v^{th} model component to $P_{II}(\mathbf{x})$ and the PhysioEnt.

$$RC_v = \sum_{\mathbf{x}} \frac{R_v(\mathbf{x})}{\sum_{\mu=1}^{10} R_{\mu}(\mathbf{x})} P_{II}(\mathbf{x}) \quad (9)$$

For the interactive components, a large RC indicates that the interaction between the associated two indexes contributes more to the BRF. Furthermore, this may suggest the BRF depends more on the corresponding physiological process. For the independent components, the larger RC indicates that the corresponding index makes a more significant independent effect on the BRF. And this may suggest that the BRF depends more on the function of the corresponding organs/tissues. In other words, the corresponding organs/tissues may be less susceptible to other organs/tissues.

3.3. Data description, preprocessing, and calculation

The dataset from Jena University Hospital is utilized, which contains the resting recordings of ECG and continuous noninvasive blood pressure of 1121 healthy individuals [54, 55]. The criterion of healthy individuals is that the individuals do not have any medical conditions,

illegal drugs or medication potentially influencing cardiovascular function. And there is no pathological finding according to thorough physical examination, resting electrocardiography and routine laboratory parameters (electrolytes, basic metabolic panel, and blood count). And the strict examination and record procedure ensure that the data can reflect the spontaneous regulation in the resting condition of healthy individuals. The labels of the dataset include age, gender and BMI. The ages range between 18 and 92 are divided into 15 groups for privacy, which are shown in Table 1.

Table 1. Age groups and corresponding ages in the dataset.

Age group	1	2	3	4	5
Age/years	18~19	20~24	25~29	30~34	35~39
Age group	6	7	8	9	10
Age/years	40~44	45~49	50~54	55~59	60~64
Age group	11	12	13	14	15
Age/years	65~69	70~74	75~79	80~84	85~92

Original data contains blood pressure, electrocardiosignal and corresponding time. The blood pressure is measured continuously using the vascular unloading technique [56]. In short, a cuff around the finger is controlled to maintain constant pressure, and the blood volume is recorded via photoplethysmography. With non-varying cuff pressure, the acquired blood volume can be mapped to blood pressure. The sampling frequency is 1000 Hz. We preprocess the data by the following methods to obtain BRS, SBP, HR, and HRV.

- 1) HR: First, we obtain the R-R interval $X_{R-R}^i(j)$ of each individual from the electrocardiosignal utilizing the mhrv toolbox in Matlab[57], where $X_{R-R}^i(j)$ represents the j^{th} $X_{R-R}^i(j)$ calculated R-R interval of the i^{th} individual. Corresponding time series can also be obtained from the mhrv toolbox: $\mathbf{t}^i = \{t^i(j)\}$. Then, we can calculate HR by $X_{HR}^i(j) = \frac{60}{X_{R-R}^i(j)}$. The calculation result can be expressed as $\mathbf{X}_{HR}^i = \{X_{HR}^i(j)\}$.
- 2) SBP: The maximum value of the blood pressure signal between $t^i(j)$ and $t^i(j+1)$ is taken as $X_{SBP}^i(j)$, and consequently $\mathbf{X}_{SBP}^i = \{X_{SBP}^i(j)\}$.
- 3) HRV: HRV can be calculated as the standard deviation of R-R intervals[58]. Therefore, we set a time window T_{HRV} and calculate HRV in T_{HRV} . First, for $t^i(j)$, we check the time points before and after $t^i(j)$, and find the time points $t^i(j-p)$ and $t^i(j+q)$ satisfying $t^i(j+q) - t^i(j) \geq \frac{T_{HRV}}{2}$ and $t^i(j) - t^i(j-p) \geq \frac{T_{HRV}}{2}$. Therefore, $t^i(j)$ can be approximate to the midpoint of the time window from $t^i(j-p)$ to $t^i(j+q)$. And the standard deviation of the R-R intervals from $t^i(j-p)$ to $t^i(j+q)$ is utilized as HRV at $t^i(j)$. As a result, each $t^i(j)$ corresponds to a time window and its HRV, and finally we obtain $\mathbf{X}_{HRV}^i = \{X_{HRV}^i(j)\}$. T_{HRV} is set as 10s [58].
- 4) BRS: BRS can be calculated in frequency domain by Eq .9 [59]:

$$X_{BRS}^i(j) = \left(\frac{p_{RRI}^i(j)}{p_{SBP}^i(j)} \right)^{\frac{1}{2}} \quad (10)$$

where: $p_{RRI}^i(j)$ and $p_{SBP}^i(j)$ are the spectral powers of R-R interval and SBP respectively from 0.07 Hz to 0.14 Hz. Therefore, we also set a time window T_{BRS} to calculate BRS. First, for $t^i(j)$, $t^i(j-p)$ and $t^i(j+q)$ are identified respectively, which satisfies $t^i(j+q) - t^i(j) \geq \frac{T_{BRS}}{2}$ and $t^i(j) - t^i(j-p) \geq \frac{T_{BRS}}{2}$. Then the spectral powers of R-R interval and SBP from $t^i(j-p)$ to $t^i(j+q)$ are calculated to deduce $X_{BRS}^i(j)$, and finally $\mathbf{X}_{BRS}^i = \{X_{BRS}^i(j)\}$. T_{BRS} is set as 120s [59].

To calculate the PhysioEnt of the indexes, the normalization is conducted first according to Eq. 11, which aims to eliminate the influence of the dimensions of indexes:

$$\begin{aligned} x_{\text{BRS}}^i(j) &= \frac{X_{\text{BRS}}^i(j) - \min\{\mathbf{X}_{\text{BRS}}^i\}}{\max\{\mathbf{X}_{\text{BRS}}^i\} - \min\{\mathbf{X}_{\text{BRS}}^i\}}, x_{\text{SBP}}^i(j) = \frac{X_{\text{SBP}}^i(j) - \min\{\mathbf{X}_{\text{SBP}}^i\}}{\max\{\mathbf{X}_{\text{SBP}}^i\} - \min\{\mathbf{X}_{\text{SBP}}^i\}}, \\ x_{\text{HR}}^i(j) &= \frac{X_{\text{HR}}^i(j) - \min\{\mathbf{X}_{\text{HR}}^i\}}{\max\{\mathbf{X}_{\text{HR}}^i\} - \min\{\mathbf{X}_{\text{HR}}^i\}}, x_{\text{HRV}}^i(j) = \frac{X_{\text{HRV}}^i(j) - \min\{\mathbf{X}_{\text{HRV}}^i\}}{\max\{\mathbf{X}_{\text{HRV}}^i\} - \min\{\mathbf{X}_{\text{HRV}}^i\}} \end{aligned} \quad (11)$$

where $x_{\text{BRS}}^i(j)$, $x_{\text{SBP}}^i(j)$, $x_{\text{HR}}^i(j)$, $x_{\text{HRV}}^i(j)$ represent the j^{th} normalized BRS, SBP, HR and HRV data of the i^{th} individual, respectively.

For the discretization of the normalized data, the value space of each index is coarse grained into 10 uniform levels from 0 to 1, and the continuous-valued data points are assigned the midpoints of the levels they fall into. For instance, the data points falling into $[0, 0.1)$, $[0.1, 0.2)$, and $[0.2, 0.3)$ are assigned 0.05, 0.15, and 0.25 respectively.

Based on the data preprocessing procedure, the PhysioEnts of $P_{\text{II}}(\mathbf{x})$, $P_{\text{III}}(\mathbf{x})$, and $P_{\text{IV}}(\mathbf{x})$ for 1058 individuals are calculated separately, in which we censor the data of 63 volunteers with large estimation errors or missing labels. And the corresponding multi-information ratios are calculated as well. The averaged multi-information ratios of 1058 individuals for $P_{\text{II}}(\mathbf{x})$, $P_{\text{III}}(\mathbf{x})$, and $P_{\text{IV}}(\mathbf{x})$ are 0.8810, 0.8822, and 0.8832, respectively. It means that these models can effectively represent more than 88% of the information embedded in the data, and there is no significant difference among them. Therefore, $P_{\text{II}}(\mathbf{x})$ can represent the observed data well enough. It might provide some evidence and support for why the current physiological and medical researches focus on the pairwise correlations between physiological indexes. And the following analysis is conducted based on $P_{\text{II}}(\mathbf{x})$, i.e. Eq. 4.

As for the stable range of the PhysioEnt to evaluate the resting-condition BRF, we calculate the 90% confidence interval of the PhysioEnt. And the 5th and 95th percentiles of data are taken as the lower bound and upper bound of the confidence interval, respectively. Since individuals are labelled with age, gender, and BMI, it can facilitate us to further explore the demographic features of the resting-condition BRF by analyzing the statistical relationships between the PhysioEnt and these three labels. For this purpose, a multivariable linear regression (see section 3.4 for details) is conducted, in which age, gender, and BMI are the independent variables and the PhysioEnt is the dependent variable. And the detailed analysis is given in section 4.1.

As for the model components' RCs in $P_{\text{II}}(\mathbf{x})$, we calculate the RCs of all model components for each individual, and a one-way ANOVA is utilized to compare the differences among the RCs (see section 3.4 for details). The detailed analysis is given in section 4.2.1.

In addition, like the PhysioEnt of the resting-condition BRF, the RCs can also be analyzed to study the demographic features of specific physiological processes and organs/tissues. Multivariable linear regressions are conducted, in which age, gender, and BMI are the independent variables and the RCs are the dependent variables. And the detailed analyses are given in sections 4.2.2 and 4.2.3 respectively.

3.4. Statistical analysis

Multivariable linear regression is adopted to analyze the statistical relationships between the PhysioEnt and the three labels, i.e. age, gender, and BMI; and the relationships between the RCs and such labels. For the regression results, the F-test is performed to verify whether the regression model is statistically significant; and the t-test is performed to identify the significance of the effect of each label.

One-way ANOVA is utilized to verify the differences among the different model components' RCs . First, the Levene's test is performed to test the homoscedasticity of the RCs .

The statistical result shows the p value of the Levene's test is less than $1E-10$, which indicates that the different model components' RCs are significantly heteroscedastic. Therefore, we adopt the two-tailed Games-Howell test for pairwise comparisons.

All statistical analyses are performed using IBM SPSS Statistics.

4. Results

4.1. The demographic features of the resting-condition BRF

According to the statistical regression between the PhysioEnt and age, gender, and BMI, there is a significant negative correlation between age and the PhysioEnt and a significant positive correlation between BMI and the PhysioEnt, while gender has no significant effect on the PhysioEnt. In other words, younger people and the people with higher BMI have more diverse physiological index states. Specifically, Table 2 provides the statistical results, and Figures 2 (A) and (B) provide the trends of the expectation and 90% confidence interval of the PhysioEnt with age and BMI. According to Figure 2, for the general healthy population, the expectations and 90% confidence intervals approximately keep unchanged, which supports that the PhysioEnt is supposed to remain in a stable range for healthy individuals. For the trends of the PhysioEnt with age and BMI, these are further discussed in section 5.1.

Table 2. Multivariable linear regression results between the PhysioEnt and demographic labels. F is the F value of the F -test for the regression. $p^{F\text{-test}}$ is the p value of the F -test. β_{age}^* , β_{gender}^* and β_{BMI}^* are the standardized regression coefficients of age, gender and BMI respectively; t_{age} , t_{gender} and t_{BMI} are the t values of t -test for age, gender and BMI; $p_{\text{age}}^{t\text{-test}}$, $p_{\text{gender}}^{t\text{-test}}$ and $p_{\text{BMI}}^{t\text{-test}}$ are the p values of t -test for age, gender, and BMI. The p values less than 0.05 are marked with *.

The statistical results of the F test		
F		$p^{F\text{-test}}$
9.217		0.000005*
The statistical results of t test		
β_{age}^*	β_{gender}^*	β_{BMI}^*
-0.169	-0.009	0.088
t_{age}	t_{gender}	t_{BMI}
-5.180	-0.294	2.669
$p_{\text{age}}^{t\text{-test}}$	$p_{\text{gender}}^{t\text{-test}}$	$p_{\text{BMI}}^{t\text{-test}}$
2.662E-7*	0.769	0.00773*

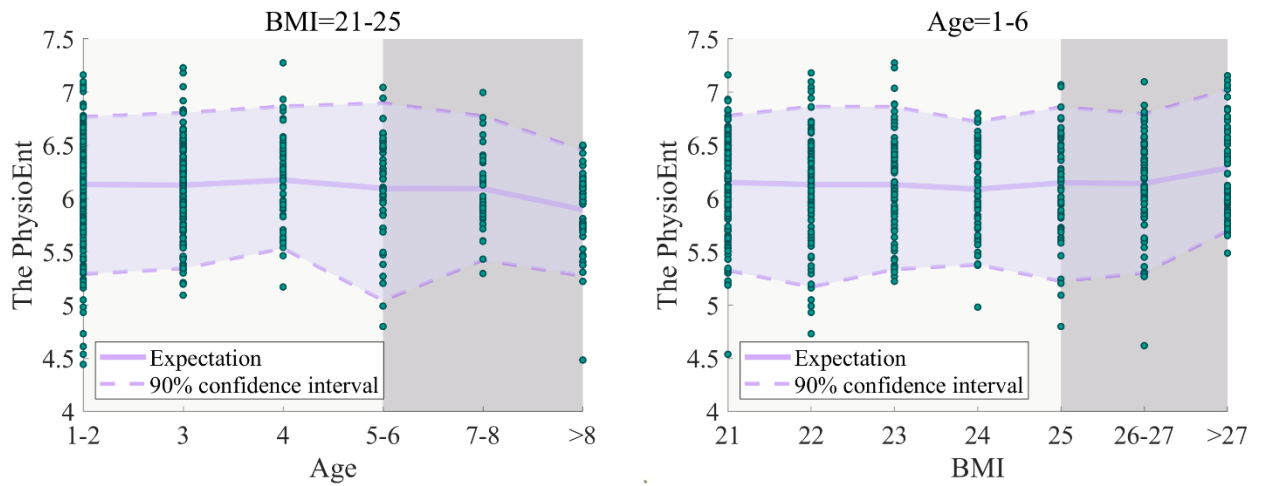


Figure 2. (A, left): Trend of the expectation and 90% confidence interval of the PhysioEnt with age. The areas with white backgrounds represent the range of the general healthy population, i.e. the individuals with age group 1-6 and BMI group 21-25 [60]; and the areas with grey backgrounds represent the range of the individuals with age group >6 or BMI >25. (B, right): Trend of the expectation and 90% confidence interval of the PhysioEnt with BMI.

4.2. The effects of the physiological processes and organs/tissues on the resting-condition BRF

4.2.1. The comparisons among the physiological processes and organs/tissues

The statistical results of the one-way ANOVA indicate that there are significant differences in the *RCs* of most model components (see Table S1 and S2 in Supplementary materials for details). Figure 3 provides the qualitative comparisons among the different model components' *RCs* for various age and gender groups. These results show that in each age and gender group, the sum of all interactive components' *RCs*, i.e. the sum of green parts, is greater than the sum of all independent components' *RCs*, i.e. the sum of purple parts. This indicates the interactions among indexes contribute more to the resting-condition BRF compared with independent indexes. Further, this suggests that the resting-condition BRF depends more on the stability of the physiological processes than the functions of organs/tissues for all populations.

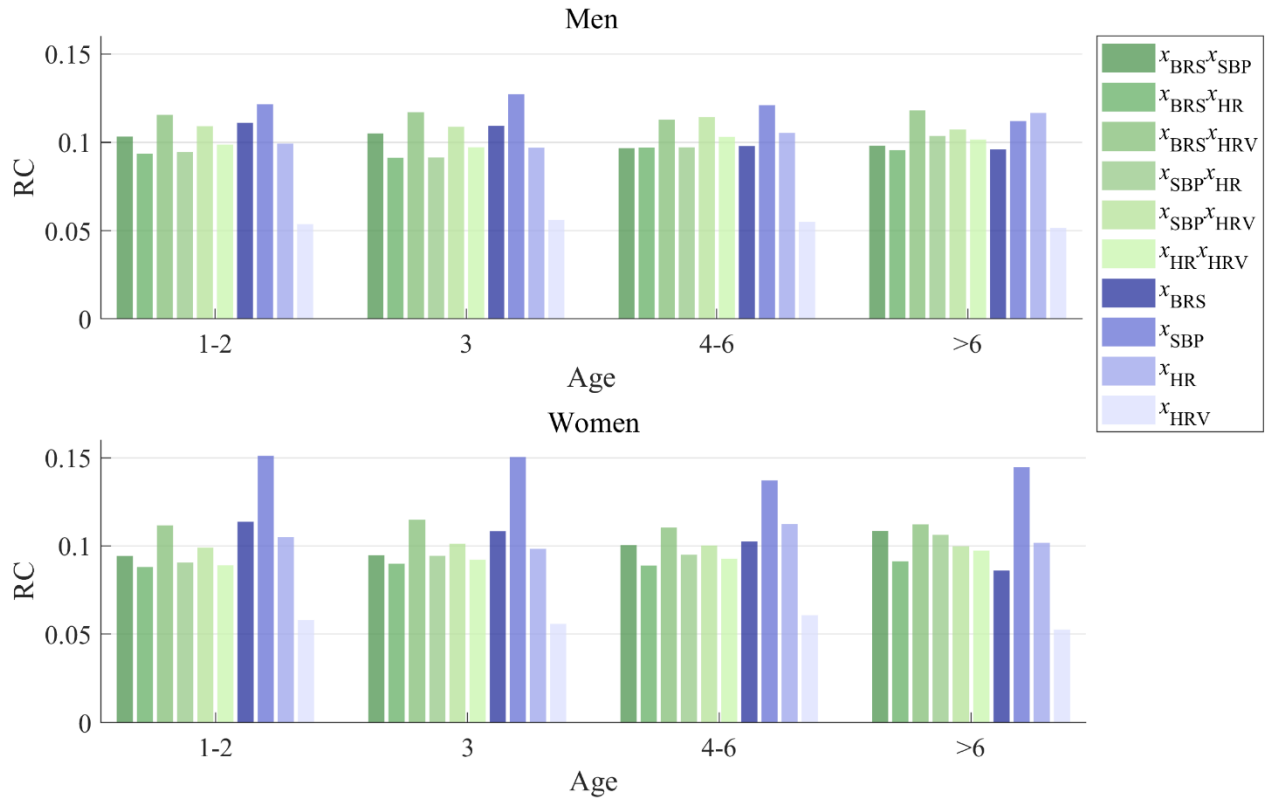


Figure 3. Comparisons among the different model components' RC s in various groups. In each age and gender group, there are 10 boxes corresponding to the expectations of 10 model components' RC s. On the one hand, the comparisons among different model components' RC s in each group are provided; on the other hand, for one model component's RC , its trend in different age and gender groups can be reflected.

In addition, among the interactive components, the RC of $x_{BRS}x_{HRV}$ is the largest one in all gender and age groups while the RC of $x_{BRS}x_{HR}$ is the smallest one. Among the independent components, the RC of x_{SBP} is the largest in most gender and age groups and the RC of x_{HRV} is the smallest one. These are further discussed in section 5.2.1.

Further, there are obvious differences in different age and gender groups. The interactive components of older people contribute more than those of younger people. And the interactive components of men contribute more than those of women. In contrast, the independent components show opposite trends with age and gender, compared with the interactive components. The detailed analyses are given in sections 4.2.2 and 4.2.3.

4.2.2. The age differences in the physiological processes and organs/tissues

For the sum of the interactive components' RC s and the sum of the independent ones, the results of regression show that they both have significant correlations with age and gender, and the statistical results are provided in Table 3. As for the correlations of these sums with age, the trends of the expectations and 90% confidence intervals are shown in Figures 4 (A) and (B). These results show that the sum of the interactive components' RC s increases with age, and the sum of the independent components' RC s decreases with age. These indicate that for older people, the interactions among indexes contribute more to the resting-condition BRF.

Table 3. Multivariable linear regression results between the RC s' sums and demographic labels.

The statistical results of the F test		
Model components	the sum of the interactive components	the sum of the independent components
F	10.433	10.433

$p^{F\text{-test}}$	9.103E-7*	9.103E-7*
The statistical results of t test		
Model components	the sum of the interactive components	the sum of the independent components
β_{age}^*	0.0941	-0.0941
β_{gender}^*	-0.135	0.135
β_{BMI}^*	-0.000084	0.000084
t_{age}	2.884	-2.884
t_{gender}	-4.400	4.400
t_{BMI}	-0.00254	0.00254
$p_{\text{age}}^{\text{t-test}}$	0.004*	0.004*
$p_{\text{gender}}^{\text{t-test}}$	0.000012*	0.000012*
$p_{\text{BMI}}^{\text{t-test}}$	0.998	0.998

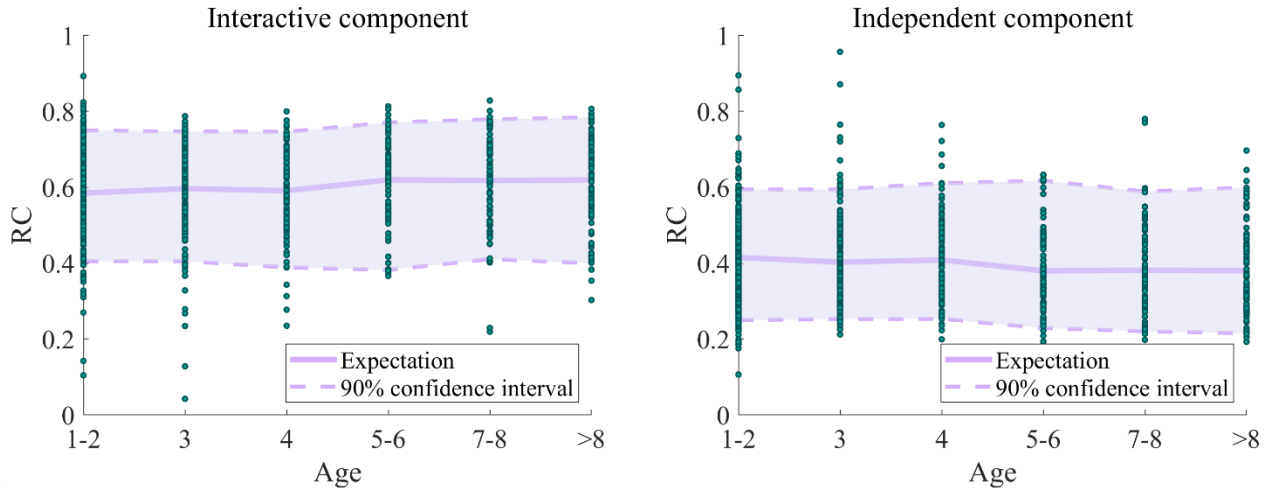


Figure 4. (A, left): Trend of the expectation and 90% confidence interval of the sum of the interactive components' RCs with age. (B, right): Trend of the expectation and 90% confidence interval of the sum of the independent components' RCs with age.

For each model components' RCs, the results of regression show that the RCs of $x_{\text{SBP}}x_{\text{HR}}$, $x_{\text{HR}}x_{\text{HRV}}$, and x_{BRS} have significant correlations with age; and the RCs of $x_{\text{BRS}}x_{\text{HR}}$, $x_{\text{HR}}x_{\text{HRV}}$, $x_{\text{SBP}}x_{\text{HRV}}$, and x_{SBP} have significant correlations with gender. The specific statistical results are provided in Table 4. As for the model components' RCs that change with age significantly, the trends of the expectations and 90 % confidence intervals with age are shown in Figures 5 (A)-(C).

Table 4. Multivariable linear regression results between the model components' RCs and demographic labels.

The statistical results of the F test		
Model component	F	$p^{F\text{-test}}$
$x_{\text{BRS}}x_{\text{SBP}}$	0.952	0.415
$x_{\text{BRS}}x_{\text{HR}}$	6.284	0.000316*
$x_{\text{BRS}}x_{\text{HRV}}$	1.251	0.290
$x_{\text{SBP}}x_{\text{HR}}$	11.123	3.436E-7*
$x_{\text{SBP}}x_{\text{HRV}}$	12.291	6.602E-8*
$x_{\text{HR}}x_{\text{HRV}}$	12.171	7.815E-8*

x_{BRS}	5.915	0.000530*				
x_{SBP}	5.624	0.000797*				
x_{HR}	1.201	0.308				
x_{HRV}	1.993	0.113				
The statistical results of t test						
Model component	β_{age}^*	β_{gender}^*	β_{BMI}^*			
$x_{BRS}x_{SBP}$	0.0368	-0.0270	-0.0107			
$x_{BRS}x_{HR}$	0.0582	-0.119	-0.0151			
$x_{BRS}x_{HRV}$	-0.00562	-0.0434	0.0371			
$x_{SBP}x_{HR}$	0.180	-0.0250	-0.0261			
$x_{SBP}x_{HRV}$	0.00188	-0.185	-0.00969			
$x_{HR}x_{HRV}$	0.104	-0.150	-0.022			
x_{BRS}	-0.122	0.00354	-0.0147			
x_{SBP}	-0.0151	0.119	-0.0167			
x_{HR}	0.00999	0.0101	0.0545			
x_{HRV}	-0.0271	0.0445	-0.0388			
Model component	t_{age}	t_{gender}	t_{BMI}	p_{age}^{t-test}	p_{gender}^{t-test}	p_{BMI}^{t-test}
$x_{BRS}x_{SBP}$	1.112	-0.868	-0.321	0.266	0.386	0.748
$x_{BRS}x_{HR}$	1.774	-3.854	-0.458	0.0763	0.000123*	0.647
$x_{BRS}x_{HRV}$	-0.170	-1.398	1.114	0.865	0.162	0.265
$x_{SBP}x_{HR}$	5.518	-0.816	-0.795	4.30E-8*	0.415	0.427
$x_{SBP}x_{HRV}$	0.0577	-6.045	-0.296	0.954	2.073E-9*	0.768
$x_{HR}x_{HRV}$	3.203	-4.906	-0.672	0.00140*	0.000001*	0.501
x_{BRS}	-3.721	0.115	-0.444	0.000209*	0.909	0.657
x_{SBP}	-0.460	3.870	-0.504	0.646	0.000116*	0.614
x_{HR}	0.302	0.326	1.637	0.762	0.744	0.102
x_{HRV}	-0.821	1.435	-1.167	0.412	0.152	0.243

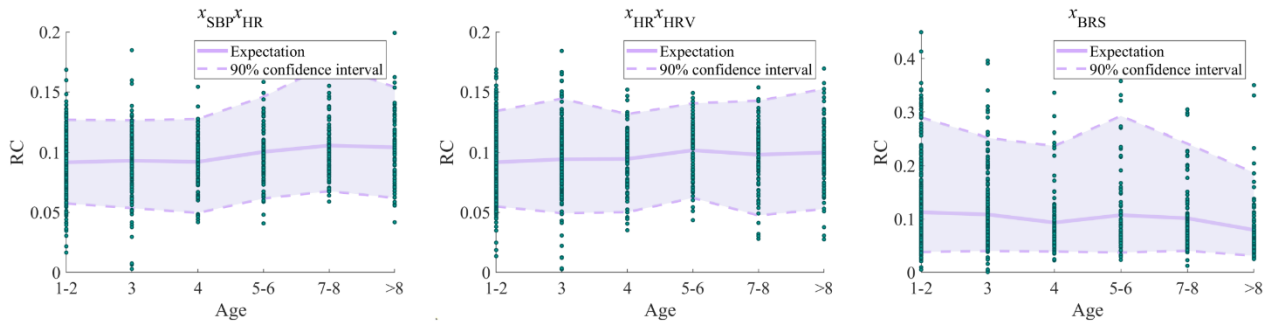


Figure 5. (A, left): Trend of the expectation and 90% confidence interval of the RC of $x_{SBP}x_{HR}$ with age. (B, middle): Trend of the expectation and 90% confidence interval of the RC of $x_{HR}x_{HRV}$ with age. (C, right): Trend of the expectation and 90% confidence interval of the RC of x_{BRS} with age.

For the results in this section, the further discussions are provided in section 5.2.2.

4.2.3. The gender differences in the physiological processes and organs/tissues

According to Table 3, the sum of the interactive components' RCs and the sum of the independent ones both have significant correlations with gender, and Figures 6 (A) and (B) provide the boxplots of men and women. Specifically, for the sum of the interactive components' RCs , the one of men is larger than the one of women; and for the sum of the independent components' RCs , the one of women is larger than the one of men. These results indicate that the physiological processes of men contribute more to their resting-condition BRF than those of women, and the organs/tissues of women contribute more than those of men.

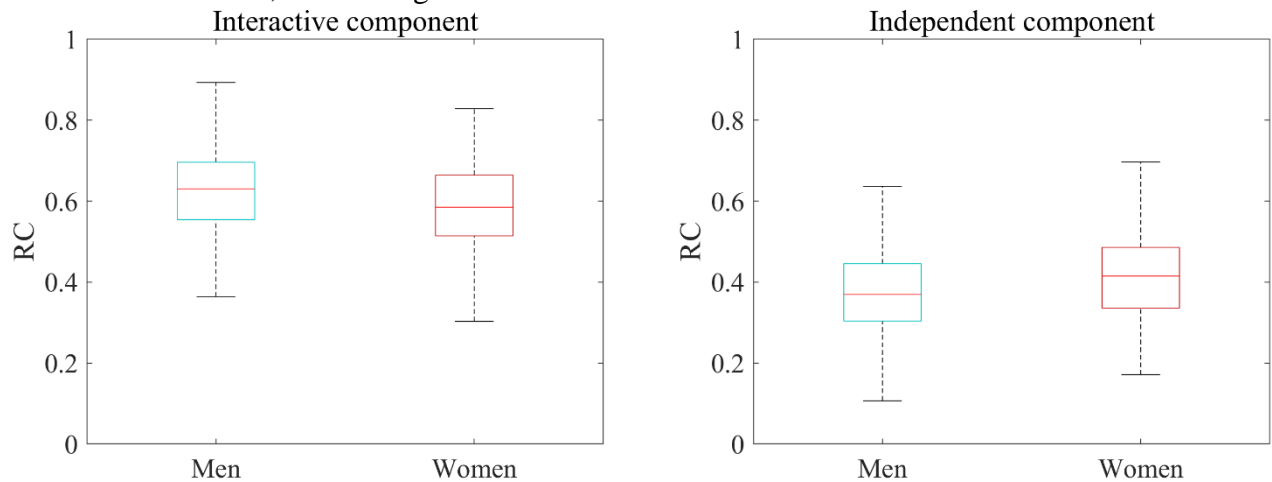


Figure 6. (A, left): Boxplot of the sum of the interactive components' RCs in men and women. (B, right): Boxplot of the sum of the independent components' RCs in men and women.

As for the model components' RCs that have significant relationships with gender, i.e. the RCs of $x_{BRS}x_{HR}$, $x_{HR}x_{HRV}$, $x_{SBP}x_{HRV}$, and x_{SBP} , the boxplots for men and women are shown in Figures 7 (A)-(D). Similarly, for the results in this section, the further discussions are provided in section 5.2.3.

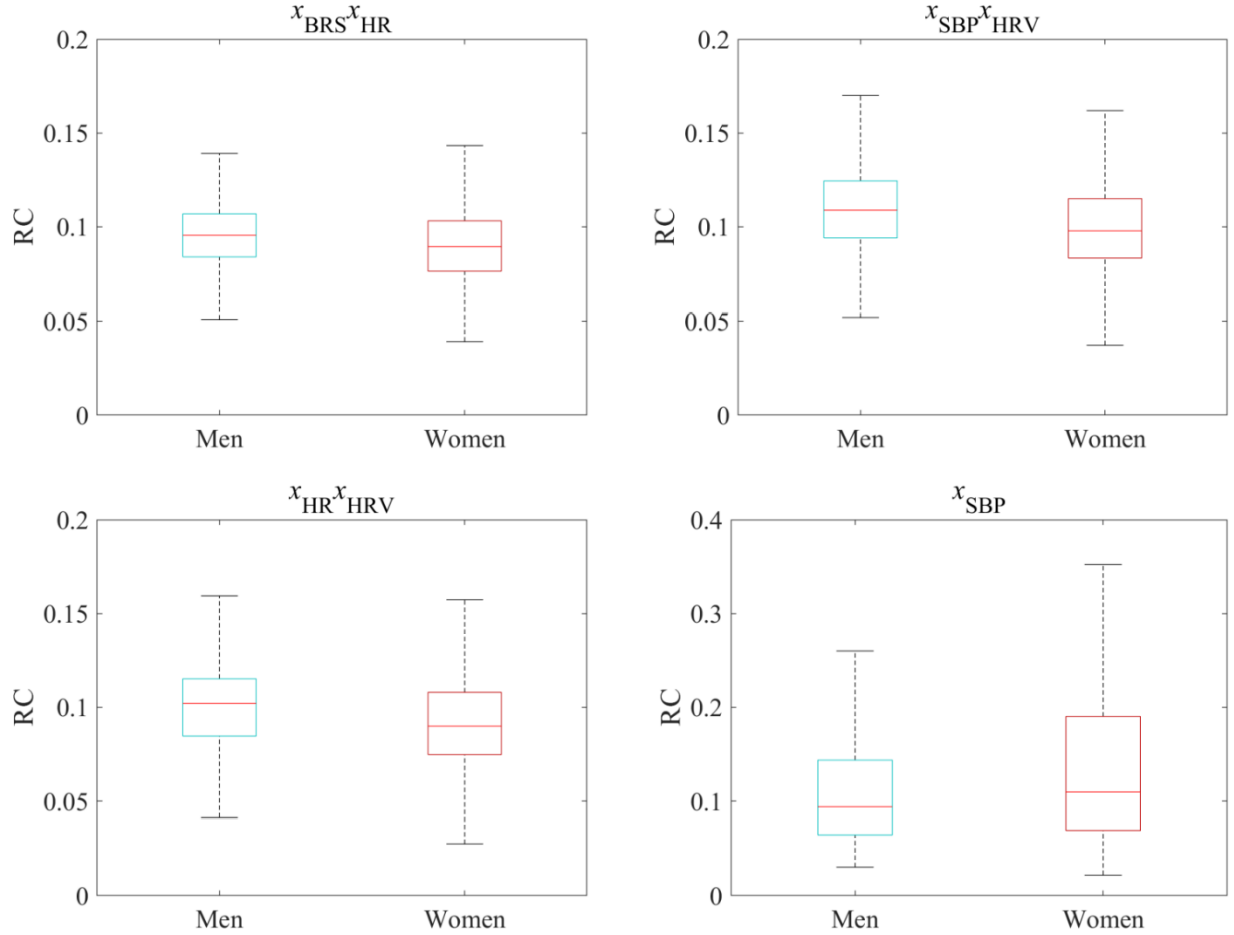


Figure 7. (A, upper left) Boxplot of the RC of $x_{BRS}x_{HR}$ in men and women. (B, upper right): Boxplot of the RC of $x_{HR}x_{HRV}$ in men and women. (C, lower left): Boxplot of the RC of $x_{SBP}x_{HRV}$ in men and women. (D, lower right): Boxplot of the RC of x_{SBP} in men and women.

5. Discussion

5.1. Different mechanisms that aging and obesity affect the resting-condition BRF

According to section 4.1, the PhysioEnt decreases with age and increases with BMI. These trends may suggest that:

- 1) The decrease in older people and the increase in the people with higher BMI may suggest that the resting-condition BRF is significantly different for such individuals compared with the general healthy population. Current medical researches also identify the weakening of BRF with aging and obesity [61, 62]. In addition, the opposite trends of the PhysioEnt with age and BMI may suggest different physiological mechanisms.
- 2) For the decrease of the PhysioEnt with aging: It has been found that the hardening of arteries weakens BRF with aging [63]. Since the individuals in the dataset of our work do not have any pathologic condition [54], with aging, there might be a self-adaptation for the human body; and then, the states of physiological indexes become less diverse to adapt to the weakening BRF. This process may suggest it is a feature of the normal aging, but it also suggests that the BRFs of old people are not as healthy as the ones of young people.
- 3) For the increase of the PhysioEnt with BMI: Relatively high BMI is generally considered to be an unhealthy state. Even though the individuals do not have cardiovascular-related

pathologic conditions, obesity may also have an adverse effect on the autonomic nerves [64]. Therefore, this result may indicate that the BRF of the people with higher BMI is weaker, and the states of physiological indexes may be more unstable due to the reasons like disturbances in autonomic activities. This suggests that the increase PhysioEnt with BMI should be paid more attention to healthcare.

5.2. The effects of the physiological processes and organs/tissues on the resting-condition BRF

5.2.1. Organs/tissues and physiological processes contributing significantly to the resting-condition BRF

According to section 4.2.1, the RC s of some components are significantly large or small. These may imply that:

- 1) The RC of $x_{BRS}x_{HRV}$ is the largest compared with the other interactive components in all gender and age groups. This indicates that the interaction between the BRS and the HRV contributes the most to the resting-condition BRF compared with other interactions. Further, this may suggest that parasympathetic regulation affects the resting-condition BRF most significantly in all physiological processes. This result is consistent with current researches that the diseases related to parasympathetic nerves usually result in the severe fluctuations of indexes [65-67].
- 2) The RC of $x_{BRS}x_{HR}$ is the smallest compared with the other interactive components in all gender and age groups. Since the interaction between the BRS and the HR contributes less to the resting-condition BRF and the corresponding physiological process seems to be unclear, this may suggest paying less attention to this interaction in future researches.
- 3) The RC of x_{SBP} is the largest for women in all age groups; for men, it is also relatively large, especially in age groups less than 6. This indicates the significant independent contribution of the SBP to the BRF. And this may suggest that the BRF depends more on blood vessels, and blood vessels may be less susceptible to other organs/tissues.
- 4) The RC of x_{HRV} is the smallest in all gender and age groups. This indicates the least independent contribution of HRV. HRV mainly represents the afferent parasympathetic function, and parasympathetic nerves interact a lot with other organs/tissues. This may lead to the relatively insignificant independent contribution.

5.2.2. The resting-condition BRF of old people depends more on the stability of the physiological processes

The results in section 4.2.2 show that for older people, the interactions among indexes contribute more to the resting-condition BRF. These may suggest that the resting-condition BRF of older people depends more on the stability of the physiological processes. Therefore, it may be more important to maintain the stable operation of regulation for older people. This can provide guidance for treatments to related diseases, and can also support some interventions for the old patients aiming to enhance the regulation such as stimulating the carotid sinus [68] and the parasympathetic nerves [69].

Further, the RC s of $x_{SBP}x_{HR}$, $x_{HR}x_{HRV}$, and x_{BRS} have significant correlations with age. These results suggest that:

- 1) The RC of $x_{SBP}x_{HR}$ increases with age. This indicates that for older people, the interaction between the SBP and the HR contributes more to the resting-condition BRF. And this suggests that older people depend more on the process that heart rate affects blood pressure.

Current researches also identified the degeneration of this process [70, 71]. Therefore, it is more important for old people to maintain this process stable.

- 2) The RC of $x_{HR}x_{HRV}$ increases with age. This indicates that for older people, the interaction between the HR and the HRV contributes more to the resting-condition BRF. And this suggests older people depend more on the process that parasympathetic nerves innervate heart rate. This result is also supported by some medical findings [70, 72].
- 3) The RC of x_{BRS} decreases with age, which implies the less independent effect of BRS for older people. Since x_{BRS} represents the function of efferent parasympathetic nerves, this may suggest that with aging, parasympathetic nerves interact more with other organs/tissues and leads to its less independent effect.

5.2.3. The resting-condition BRF of men depends more on the stability of the physiological processes

According to section 4.2.3, men depend more on the physiological processes than women, while women depend more on the functions of organs/tissues than men. These results may explain the gender differences in some baroreflex-related diseases. For example, it has been noted that men are more likely to die after a spontaneous intracerebral hemorrhage than women [73]. In addition, researches show that the weakening of the BRF increases the risk of acute intracerebral hemorrhage and secondary brain injury [74]. According to this section, to keep the BRF, for men, maintaining the functions of organs/tissues may not be as effective as for women. Therefore, when the failure of the BRF occurs and leads to intracerebral hemorrhage, it may be more difficult for men to restore the homeostasis of baroreflex, and this may be the explanation that the greater odds of dying for men.

Further, the RC s of $x_{BRS}x_{HR}$, $x_{HR}x_{HRV}$, $x_{SBP}x_{HRV}$, and x_{SBP} have significant correlations with gender. These results suggest that:

- 1) Men's RC of $x_{BRS}x_{HR}$ is larger, and this indicates that the interaction between the BRS and the HR contributes more to the resting-condition BRF for men. Since the relationship between the short-term HR and the BRS is not clear, the result suggests that men may depend more on related unclear physiological mechanisms.
- 2) Men's RC of $x_{HR}x_{HRV}$ is larger, and this indicates that the interaction between the HR and the HRV contributes more to the resting-condition BRF for men. And this may suggest men depend more on the process that parasympathetic nerves innervate heart rate. Some researches also reported that this process of men is less robust compared with the one of women [75, 76]. Therefore, it is more important for men to maintain this process stable.
- 3) Men's RC of $x_{SBP}x_{HRV}$ is larger, and this indicates that the interaction between the SBP and the HRV contributes more to the resting-condition BRF for men. And this may be the indirect reflection of the process related to parasympathetic nerves mentioned above.
- 4) Women's RC of x_{SBP} is larger, and this indicates the greater independent effect of the SBP for women. And this may suggest that for women, the function of blood vessels is less susceptible to other organs/tissues. This may be due to the protective effect of estrogens on blood vessels [77].

5.3. The rationale and novelty of the PhysioEnt

In this section, the rationale and novelty of the proposed PhysioEnt to quantify the BRF are further discussed. The rationale of the proposed method is, essentially, the fluctuations of the physiological indexes can represent the BRF effectively, which has been studied and proved by current physiological studies as stated in section 1. In fact, the BRS utilized generally in

clinic is also calculated based on the fluctuations of blood pressure and heart rate. However, BRS has been proved to be partial when measuring the BRF as mentioned in section 2.

Therefore, a systematic quantification of the fluctuations of indexes is expected. In addition, and more importantly, we hope that this quantification is related to specific physiological mechanisms. For these purposes, the maximum entropy model in statistical physics are adopted, and the PhysioEnt is proposed. Generally, compared with the traditional BRS, there are two major advances for the PhysioEnt:

First, and obviously, the PhysioEnt incorporates more physiological indexes than just one BRS. Therefore, as mentioned in section 2, the concerned four indexes can cover the resting-condition baroreflex and represent the resting-condition BRF. For this point, the correlations for each one of the four indexes with age, gender, and BMI are studied to verify the necessity for the PhysioEnt to combine the indexes. The statistical results are depicted in Table 5.

Table 5. Multivariable linear regression results between each one of the four indexes and demographic labels.

The statistical results of the F test						
Physiological indexes	F			$p^{F\text{-test}}$		
BRS	10.264			<1E-10*		
HRV	14.075			<1E-10*		
SBP	4.080			0.007*		
HR	7.546			0.000054*		
The statistical results of t test						
Model component	β_{age}^*		β_{gender}^*		β_{BMI}^*	
BRS	-0.171		0.009		0.010	
HRV	-0.168		0.056		-0.034	
SBP	0.044		0.099		-0.023	
HR	0.055		0.134		0.030	
Model component	t_{age}	t_{gender}	t_{BMI}	$p_{age}^{t\text{-test}}$	$p_{gender}^{t\text{-test}}$	$p_{BMI}^{t\text{-test}}$
BRS	-5.245	0.288	0.316	1.88E-7*	0.773	0.752
HRV	-5.173	1.833	-1.037	2.76E-7*	0.067	0.300
SBP	1.340	3.189	-0.699	0.181	0.001*	0.485
HR	1.674	4.364	0.919	0.094	0.000014*	0.358

Results show that: 1) there are only negative correlations for BRS and HRV with age. Both BRS and HRV represent the function of autonomic nervous system. Especially for BRS, it has been generally adopted to measure the BRF in clinic. However, the individual analysis on BRS and HRV can only find the influence of aging, but not the effect of obesity which can be cognized by the PhysioEnt. 2) there are significant gender differences for SBP and HR. It should be figured that the fluctuations but not the levels of blood pressure and heart rate, are the basis to measure the BRF [59]. Therefore, such regression results may not effectively represent the relationships between the resting-condition BRF and gender. Conclusively, by combining all four indexes, the PhysioEnt can capture more effective information about the resting-condition BRF.

Besides the necessity to combine the indexes, more importantly, as mentioned before, we expect to achieve a brief and effective systematic characterization of the complex physiological mechanisms when quantifying the resting-condition BRF. The traditional quantifications of BRF, such as BRS, are generally the observation and calculation of the changes of blood

pressure and heart rate. Such quantifications are essentially the black-box methods, which lack the description of the physiological mechanisms. Therefore, for the statistical analysis of the indexes including BRS, it is difficult to abduct the factors affecting the BRF, not even to help for improving the BRF. On the other hand, the detailed modeling and analysis on the mechanisms of baroreflex regulation are also difficult, and the complete white-box models could be complicated and unrealistic in clinical application.

To solve these problems, the maximum entropy model in statistical physics is adopted and the PhysioEnt is proposed. For the PhysioEnt, its essence is to construct a hypothetical maximum entropy model based on the physiological mechanisms in advance, and complete the model based on the observed data. When building the model, each model component corresponds to some specific part of the baroreflex regulation in advance. Therefore, the PhysioEnt can not only represent the systematic BRF, but also study the effects of specific organs/tissues and physiological processes on the BRF based on the *RC* proposed in section 3.2. Conclusively, for the PhysioEnt based on the maximum entropy model, it reflects the emergence from the bottom-layer physiological mechanisms to the middle-layer physiological indexes and the top-layer BRF, as stated in section 2.

According to the above advances, the PhysioEnt can capture some novel conclusions compared with traditional indexes like BRS. Summarized from section 5.1 and 5.2, there are two aspects of the new findings:

- 1) The mechanisms that aging and obesity affect the resting-condition BRF are different. Studies have shown that old people and obese people both have decreased BRSs. However, the proposed PhysioEnt provides a different insight: the PhysioEnt decreases with aging and increases with BMI, which may suggest different mechanisms. In fact, the physiological studies show that the mechanisms of aging and obesity affecting BRF are not exactly the same, as analyzed in section 5.1. Conclusively, such a physiological difference can be recognized by the PhysioEnt but not by BRS.
- 2) Compared with the functions of the organs/tissues, the stability of the physiological processes among the organs/tissues is more critical for the resting-condition BRF, especially for men and old people. The detailed analyses are provided in section 4.2 and 5.2. On the one hand, as mentioned in section 5.2.3, this may be corroborated by some clinical findings, such as the unclear high mortality for men after a spontaneous intracerebral hemorrhage, which may result from the fact that men are more difficult to recover from the failure of regulation due to the stronger dependencies among the organs/tissues. On the other hand, maintaining the physiological processes is more meaningful to recover and strengthen the BRF. It should be noted that such analyses that how specific physiological mechanisms affect the BRF cannot be obtained from BRS.

5.4. Limitations and prospects

In this work, the PhysioEnt emerging from the BRS, SBP, HR, and HRV is considered to represent the regulation intensity of the resting-condition baroreflex. Some new medical findings are also obtained only based on the limited data. Consequently, there must be some limitations existing in our work, mainly including the integrity of the physiological indexes and the sufficiency of the data.

As for the above four indexes, they are selected based on both the current medical knowledge and the testability. Restricted by current researches, basically, it is hard to say these four indexes can fully represent the resting-condition BRF. The corresponding PhysioEnt, hence, may not perfectly fit the resting-condition BRF. As for the sufficiency of the data, the effects of some physiological systems such as the renin-angiotensin-aldosterone system (RAAS) cannot be considered due to the lack of data. In addition, the sample sizes of the

adopted data are relatively limited and uneven after being stratified by the three labels, which may affect the accuracy of the conclusions. Also, the dataset only records the data of healthy individuals, while the analysis on the patients with some pathology may provide more interesting findings.

For the future work, based on the proposed paradigm, more physiological systems that affect the BRF will be concerned with the proper datasets. In addition, the BRF not limited to the resting condition will be focused on, which may be more meaningful to the healthcare in daily life. The data collection and analysis for patients will also be conducted to support the disease diagnosis and treatment. For such purposes, the individualized dynamic monitoring data in different conditions is required, and this would be achieved briefly with the widespread appliance of wearable devices. Prospectively, such work would support the individualized real-time evaluation for the healthy degree of the BRF, and guide the precision medicine.

Data Availability

The adopted dataset in this work is available via the physionet website (<https://physionet.org/content/autonomic-aging-cardiovascular/1.0.0/>).

Funding Statement

This work is supported by the National Natural Science Foundation of China [Grant No. 51775020], the National Natural Science Foundation of China [Grant No. 62073009], and the Beijing Natural Science Foundation of China [Grant No. 7222086].

Supplementary Materials

Supplementary Texts

The model components in $P_{II}(x)$

- 1) $x_{SBP}x_{HR}$: It reflects the process that heart rate regulates blood pressure.
- 2) $x_{HR}x_{HRV}$: It reflects that the parasympathetic nerves innervate heart rate.
- 3) $x_{SBP}x_{HRV}$: It can be regarded as a combination of the above two processes.
- 4) $x_{BRS}x_{HRV}$: Since HRV and BRS are both influenced by the parasympathetic nerves, these two indexes are positively correlated [71, 78] and change simultaneously due to the parasympathetic stimulation [79]. Therefore, $x_{BRS}x_{HRV}$ may reflect the regulation of the parasympathetic nerves.
- 5) $x_{BRS}x_{SBP}$ and $x_{BRS}x_{HR}$: The physiological mechanisms of $x_{BRS}x_{SBP}$ and $x_{BRS}x_{HR}$ may not be clear. It has been found that hypertension may lead to the weakening of regulation function [80], due to vascular sclerosis [81]. In addition, the weakened regulation also increases the risk of hypertension [78, 82]. However, the relationships between short-term SBP, HR and BRS seem not to be clear. Therefore, these interactive components may be the indirect representations of other mechanisms, or may suggest unclarified physiological associations.

As for the independent components, they characterize the function of corresponding organs/tissues, as stated in section 2.

Supplementary Tables

Table S1. Expectation differences in the RCs of every two model components according to the Games-Howell tests. The value in the i^{th} row and j^{th} column represents the result that the expected RC of the model component in the i^{th} row minus the one of the model component in the j^{th} column. Therefore, the result in the i^{th} row and j^{th} column is opposite to the one in the j^{th} row and i^{th} column.

Model component	$x_{\text{BRS}}x_{\text{SBP}}$	$x_{\text{BRS}}x_{\text{HR}}$	$x_{\text{BRS}}x_{\text{HRV}}$	$x_{\text{SBP}}x_{\text{HR}}$	$x_{\text{SBP}}x_{\text{HRV}}$	$x_{\text{HR}}x_{\text{HRV}}$	x_{BRS}	x_{SBP}	x_{HR}	x_{HRV}
$x_{\text{BRS}}x_{\text{SBP}}$	0	0.00861	-0.0169	0.00396	-0.00435	0.00406	-0.0235	-0.0416	-0.00650	0.0429
$x_{\text{BRS}}x_{\text{HR}}$	-0.00861	0	-0.0256	-0.00465	-0.0130	-0.00456	-0.0321	-0.0502	-0.0151	0.0343
$x_{\text{BRS}}x_{\text{HRV}}$	0.0169	0.0255	0	0.0208	0.0125	0.0209	-0.00663	-0.0247	0.0104	0.0598
$x_{\text{SBP}}x_{\text{HR}}$	-0.00396	0.00465	-0.0208	0	-0.00831	0.0000930	-0.0275	-0.0456	-0.0105	0.0389
$x_{\text{SBP}}x_{\text{HRV}}$	0.00435	0.0130	-0.0125	0.00831	0	0.00840	-0.0192	-0.0373	-0.00216	0.0472
$x_{\text{HR}}x_{\text{HRV}}$	-0.00406	0.00456	-0.0209	-9.30E-05	-0.00840	0	-0.0276	-0.0457	-0.0106	0.0388
x_{BRS}	0.0235	0.0321	0.00663	0.0275	0.0192	0.0276	0	-0.0181	0.0170	0.0664
x_{SBP}	0.0416	0.0502	0.0247	0.0456	0.0373	0.0457	0.0181	0	0.0351	0.0845
x_{HR}	0.00650	0.0151	-0.0104	0.0105	0.00216	0.0106	-0.0170	-0.0351	0	0.0494
x_{HRV}	-0.0429	-0.0343	-0.0598	-0.0389	-0.0472	-0.0388	-0.0664	-0.0845	-0.0494	0

References

1. Gu, F., E. B. Randall, S. Whitesall, K. Converso-Baran, B. E. Carlson, G. D. Fink, D. E. Michele and D. A. Beard. "Potential role of intermittent functioning of baroreflexes in the etiology of hypertension in spontaneously hypertensive rats." *JCI insight* 5 (2020):
2. Tang, S., L. Xiong, Y. Fan, V. C. Mok, K. S. Wong and T. W. Leung. "Stroke outcome prediction by blood pressure variability, heart rate variability, and baroreflex sensitivity." *Stroke* 51 (2020): 1317-20.
3. La Rovere, M. T., J. T. Bigger Jr, F. I. Marcus, A. Mortara, P. J. Schwartz and A. Investigators. "Baroreflex sensitivity and heart-rate variability in prediction of total cardiac mortality after myocardial infarction." *The Lancet* 351 (1998): 478-84.
4. Bealer, S. L. "Peripheral hyperosmolality reduces cardiac baroreflex sensitivity." *Autonomic Neuroscience-Basic & Clinical* 104 (2003): 25-31. 10.1016/s1566-0702(02)00265-5. <Go to ISI>://WOS:000180940700004.
5. Ogoh, S., R. M. Brothers, Q. Barnes, W. L. Eubank, M. N. Hawkins, S. Purkayastha, A. O-Yurvati and P. B. Raven. "Effects of changes in central blood volume on carotid-vasomotor baroreflex sensitivity at rest and during exercise." *Journal of Applied Physiology* 101 (2006): 68-75. 10.1152/jappphysiol.01452.2005. <Go to ISI>://WOS:000238322200014.
6. Kent, B., J. Drane, B. Blumenstein and J. Manning. "A mathematical model to assess changes in the baroreceptor reflex." *Cardiology* 57 (1972): 295-310.
7. Zamir, M., M. B. Badrov, T. D. Olver and J. K. Shoemaker. "Cardiac baroreflex variability and resetting during sustained mild effort." *Frontiers in physiology* 8 (2017): 246.
8. Kamada, K., K. Saku, T. Tohyama, T. Kawada, H. Mannoji, K. Abe, T. Nishikawa, G. Sunagawa, T. Kishi and K. Sunagawa. "Diabetes mellitus attenuates the pressure response against hypotensive stress by impairing the sympathetic regulation of the baroreflex afferent arc." *American Journal of Physiology-Heart and Circulatory Physiology* 316 (2019): H35-H44.
9. Moslehpour, M., T. Kawada, K. Sunagawa, M. Sugimachi and R. Mukkamala. "Nonlinear identification of the total baroreflex arc: Chronic hypertension model." *American Journal of Physiology-Regulatory, Integrative and Comparative Physiology* 310 (2016): R819-R27.
10. Swenne, C. A. "Baroreflex sensitivity: Mechanisms and measurement." *Netherlands Heart Journal* 21 (2013): 58-60. 10.1007/s12471-012-0346-y. <Go to ISI>://WOS:000313657200004.
11. Biaggioni, I., C. A. Shibao and J. Jordan. *Evaluation and diagnosis of afferent baroreflex failure*. 79. Am Heart Assoc, 2022, 57-59.
12. Ataee, P., G. A. Dumont, H. A. Noubari, W. T. Boyce and J. M. Ansermino. "A novel approach to the design of an artificial bionic baroreflex." Presented at 2013 35th Annual International Conference of the IEEE Engineering in Medicine and Biology Society (EMBC), 2013. IEEE, 3813-16.
13. Lau, K. D. and C. A. Figueroa. "Simulation of short-term pressure regulation during the tilt test in a coupled 3d-0d closed-loop model of the circulation." *Biomechanics and modeling in mechanobiology* 14 (2015): 915-29.
14. Canuto, D., K. Chong, C. Bowles, E. P. Dutton, J. D. Eldredge and P. Benharash. "A regulated multiscale closed - loop cardiovascular model, with applications to hemorrhage and hypertension." *International Journal for Numerical Methods in Biomedical Engineering* 34 (2018): e2975.
15. Raphan, T., B. Cohen, Y. Xiang and S. B. Yakushin. "A model of blood pressure, heart rate, and vaso-vagal responses produced by vestibulo-sympathetic activation." *Frontiers in neuroscience* 10 (2016): 96.
16. Ishbulatov, Y. M., A. S. Karavaev, A. R. Kiselev, M. A. Simonyan, M. D. Prokhorov, V. I. Ponomarenko, S. A. Mironov, V. I. Gridnev, B. P. Bezruchko and V. A. Shvartz. "Mathematical modeling of the cardiovascular autonomic control in healthy subjects during a passive head-up tilt test." *Scientific reports* 10 (2020): 1-11.
17. Bighamian, R., B. Parvinian, C. G. Scully, G. Kramer and J.-O. Hahn. "Control-oriented physiological modeling of hemodynamic responses to blood volume perturbation." *Control engineering practice* 73 (2018): 149-60.
18. Fresiello, L., B. Meyns, A. Di Molfetta and G. Ferrari. "A model of the cardiorespiratory response to aerobic exercise in healthy and heart failure conditions." *Frontiers in physiology* 7 (2016): 189.
19. Fresiello, L., A. W. Khir, A. Di Molfetta, M. Kozarski and G. Ferrari. "Effects of intra - aortic balloon pump timing on baroreflex activities in a closed - loop cardiovascular hybrid model." *Artificial organs* 37 (2013): 237-47.

20. Hammer, P. E. and J. P. Saul. "Resonance in a mathematical model of baroreflex control: Arterial blood pressure waves accompanying postural stress." *Am J Physiol Regul Integr Comp Physiol* 288 (2005): R1637-48. 10.1152/ajpregu.00050.2004. <https://www.ncbi.nlm.nih.gov/pubmed/15718393>.
21. Di Rienzo, M., G. Mancia and G. Parati. *Blood pressure and heart rate variability: Computer analysis, modelling and clinical applications*. IOs press, 1993,
22. Berger, R. D., J. P. Saul and R. J. Cohen. "Transfer function analysis of autonomic regulation. I. Canine atrial rate response." *American Journal of Physiology-Heart and Circulatory Physiology* 256 (1989): H142-H52.
23. Porta, A., A. Marchi, V. Bari, B. De Maria, M. Esler, E. Lambert and M. Baumert. "Assessing the strength of cardiac and sympathetic baroreflex controls via transfer entropy during orthostatic challenge." *Philosophical Transactions of the Royal Society A: Mathematical, Physical and Engineering Sciences* 375 (2017): 20160290.
24. Liu, W.-M., H.-R. Liu, P.-W. Chen, H.-R. Chang, C.-M. Liao and A.-B. Liu. "Novel application of multiscale cross-approximate entropy for assessing early changes in the complexity between systolic blood pressure and ecg rr intervals in diabetic rats." *Entropy* 24 (2022): 473.
25. Diao, C. and N. Cai. "Temporal variation measure analysis: An improved second-order difference plot." *Complexity* 2022 (2022):
26. Wang, B., D. Liu, X. Gao and Y. Luo. "Three-dimensional poincaré plot analysis for heart rate variability." *Complexity* 2022 (2022):
27. Barajas-Martínez, A., E. Ibarra-Coronado, M. P. Sierra-Vargas, I. Cruz-Bautista, P. Almeda-Valdes, C. A. Aguilar-Salinas, R. Fossion, C. R. Stephens, C. Vargas-Dominguez and O. G. Atzatz-Aguilar. "Physiological network from anthropometric and blood test biomarkers." *Frontiers in physiology* (2021): 1791.
28. Cloarec - Blanchard, L. "Heart rate and blood pressure variability in cardiac diseases: Pharmacological implications." *Fundamental & clinical pharmacology* 11 (1997): 19-28.
29. Nikolaou, F., C. Orphanidou, P. Papakyriakou, K. Murphy, R. G. Wise and G. D. Mitsis. "Spontaneous physiological variability modulates dynamic functional connectivity in resting-state functional magnetic resonance imaging." *Philosophical Transactions of the Royal Society A: Mathematical, Physical and Engineering Sciences* 374 (2016): 20150183.
30. Meyer, M. and O. Stiedl. "Self-affine fractal variability of human heartbeat interval dynamics in health and disease." *European Journal of Applied Physiology* 90 (2003): 305-16.
31. He, B. J., J. M. Zempel, A. Z. Snyder and M. E. Raichle. "The temporal structures and functional significance of scale-free brain activity." *Neuron* 66 (2010): 353-69.
32. Pittman - Polletta, B. R., F. A. Scheer, M. P. Butler, S. A. Shea and K. Hu. "The role of the circadian system in fractal neurophysiological control." *Biological Reviews* 88 (2013): 873-94.
33. Hu, K., P. C. Ivanov, Z. Chen, M. F. Hilton, H. E. Stanley and S. A. Shea. "Non-random fluctuations and multi-scale dynamics regulation of human activity." *Physica A: Statistical Mechanics and its Applications* 337 (2004): 307-18.
34. Amaral, L. A. N., P. C. Ivanov, N. Aoyagi, I. Hidaka, S. Tomono, A. L. Goldberger, H. E. Stanley and Y. Yamamoto. "Behavioral-independent features of complex heartbeat dynamics." *Physical Review Letters* 86 (2001): 6026.
35. Chiesa, J. J., T. Cambras, Á. R. Carpentieri and A. Díez-Noguera. "Arrhythmic rats after scn lesions and constant light differ in short time scale regulation of locomotor activity." *Journal of biological rhythms* 25 (2010): 37-46.
36. Hu, K., F. A. Scheer, R. M. Buijs and S. A. Shea. "The circadian pacemaker generates similar circadian rhythms in the fractal structure of heart rate in humans and rats." *Cardiovascular research* 80 (2008): 62-68.
37. Cohen, A. A., L. Ferrucci, T. Fülöp, D. Gravel, N. Hao, A. Kriete, M. E. Levine, L. A. Lipsitz, M. G. Olde Rikkert and A. Rutenberg. "A complex systems approach to aging biology." *Nature Aging* 2 (2022): 580-91.
38. Balch, T. "Hierarchic social entropy: An information theoretic measure of robot group diversity." *Autonomous robots* 8 (2000): 209-38.
39. Zachary, D. and S. Dobson. "Urban development and complexity: Shannon entropy as a measure of diversity." *Planning Practice & Research* 36 (2021): 157-73.
40. Mora, T., A. M. Walczak, W. Bialek and C. G. Callan, Jr. "Maximum entropy models for antibody diversity." *Proc Natl Acad Sci U S A* 107 (2010): 5405-10. 10.1073/pnas.1001705107. <https://www.ncbi.nlm.nih.gov/pubmed/20212159>.

41. Dutoit, A. P., E. C. Hart, N. Charkoudian, B. G. Wallin, T. B. Curry and M. J. Joyner. "Cardiac baroreflex sensitivity is not correlated to sympathetic baroreflex sensitivity within healthy, young humans." *Hypertension* 56 (2010): 1118-23.
42. Kemp, A. H., J. Koenig and J. F. Thayer. "From psychological moments to mortality: A multidisciplinary synthesis on heart rate variability spanning the continuum of time." *Neuroscience & Biobehavioral Reviews* 83 (2017): 547-67.
43. Chapleau, M. W. and R. Sabharwal. "Methods of assessing vagus nerve activity and reflexes." *Heart failure reviews* 16 (2011): 109-27.
44. Huang, C., R. Gevartz, J. Onton and J. R. Criado. "Investigation of vagal afferent functioning using the heartbeat event related potential." *International Journal of Psychophysiology* 131 (2018): 113-23.
45. Nichols, W. W. and D. G. Edwards. "Arterial elastance and wave reflection augmentation of systolic blood pressure: Deleterious effects and implications for therapy." *Journal of cardiovascular pharmacology and therapeutics* 6 (2001): 5-21.
46. O'Rourke, M. "Arterial stiffness, systolic blood pressure, and logical treatment of arterial hypertension." *Hypertension* 15 (1990): 339-47.
47. Jaynes, E. T. "Information theory and statistical mechanics." *Physical review* 106 (1957): 620.
48. Jaynes, E. T. "Information theory and statistical mechanics. Ii." *Physical review* 108 (1957): 171.
49. Marsh, C. "Introduction to continuous entropy." *Department of Computer Science, Princeton University* 1034 (2013):
50. Stein, R. R., D. S. Marks and C. Sander. "Inferring pairwise interactions from biological data using maximum-entropy probability models." *PLoS computational biology* 11 (2015): e1004182.
51. Watanabe, T., S. Hirose, H. Wada, Y. Imai, T. Machida, I. Shirouzu, S. Konishi, Y. Miyashita and N. Masuda. "A pairwise maximum entropy model accurately describes resting-state human brain networks." *Nat Commun* 4 (2013): 1370. 10.1038/ncomms2388. <https://www.ncbi.nlm.nih.gov/pubmed/23340410>.
52. Darroch, J. N. and D. Ratcliff. "Generalized iterative scaling for log-linear models." *The annals of mathematical statistics* (1972): 1470-80.
53. Schneidman, E., S. Still, M. J. Berry and W. Bialek. "Network information and connected correlations." *Physical Review Letters* 91 (2003): 238701.
54. Schumann, A. and K.-J. Bär. "Autonomic aging—a dataset to quantify changes of cardiovascular autonomic function during healthy aging." *Scientific Data* 9 (2022): 1-5.
55. Goldberger, A. L., L. A. Amaral, L. Glass, J. M. Hausdorff, P. C. Ivanov, R. G. Mark, J. E. Mietus, G. B. Moody, C.-K. Peng and H. E. Stanley. "Physiobank, physiokit, and physionet: Components of a new research resource for complex physiologic signals." *Circulation* 101 (2000): e215-e20.
56. Fortin, J., W. Marte, R. Grüllenberger, A. Hacker, W. Habenbacher, A. Heller, C. Wagner, P. Wach and F. Skrabal. "Continuous non-invasive blood pressure monitoring using concentrically interlocking control loops." *Computers in Biology and Medicine* 36 (2006): 941-57.
57. Behar, J. A., A. A. Rosenberg, I. Weiser-Bitoun, O. Shemla, A. Alexandrovich, E. Konyukhov and Y. Yaniv. "Physiozoo: A novel open access platform for heart rate variability analysis of mammalian electrocardiographic data." *Frontiers in physiology* (2018): 1390.
58. Hamilton, R. M., P. S. Mckechnie and P. W. Macfarlane. "Can cardiac vagal tone be estimated from the 10-second ecg?" *International journal of cardiology* 95 (2004): 109-15.
59. Parati, G., M. Di Rienzo and G. Mancia. "How to measure baroreflex sensitivity: From the cardiovascular laboratory to daily life." *Journal of hypertension* 18 (2000): 7-19.
60. Damsgaard, C. T., K. F. Michaelsen, D. Molbo, E. L. Mortensen and T. Sørensen. "Trends in adult body-mass index in 200 countries from 1975 to 2014: A pooled analysis of 1698 population-based measurement studies with 19.2 million participants." *Lancet* 387 (2016): 1377-96.
61. Skrapari, I., N. Tentolouris and N. Katsilambros. "Baroreflex function: Determinants in healthy subjects and disturbances in diabetes, obesity and metabolic syndrome." *Current diabetes reviews* 2 (2006): 329-38.
62. Seals, D. R., K. D. Monahan, C. Bell, H. Tanaka and P. P. Jones. "The aging cardiovascular system: Changes in autonomic function at rest and in response to exercise." *International journal of sport nutrition and exercise metabolism* 11 (2001): S189-S95.
63. Monahan, K. D., H. Tanaka, F. A. Dinunno and D. R. Seals. "Central arterial compliance is associated with age-and habitual exercise-related differences in cardiovagal baroreflex sensitivity." *Circulation* 104 (2001): 1627-32.
64. Skrapari, I., N. Tentolouris, D. Perrea, C. Bakoyiannis, A. Papazafropoulou and N. Katsilambros. "Baroreflex sensitivity in obesity: Relationship with cardiac autonomic nervous system activity." *Obesity* 15 (2007): 1685-93.

65. Norcliffe-Kaufmann, L. "The vagus and glossopharyngeal nerves in two autonomic disorders." *Journal of Clinical Neurophysiology* 36 (2019): 443-51.
66. Norcliffe-Kaufmann, L., F. Axelrod and H. Kaufmann. "Afferent baroreflex failure in familial dysautonomia." *Neurology* 75 (2010): 1904-11.
67. Iio, K., S. Sakurai, T. Kato, S. Nishiyama, T. Hata, E. Mawatari, C. Suzuki, K. Takekoshi, K. Higuchi and T. Aizawa. "Endomyocardial biopsy in a patient with hemorrhagic pheochromocytoma presenting as inverted takotsubo cardiomyopathy." *Heart and vessels* 28 (2013): 255-63.
68. Scheffers, I. J., A. A. Kroon, J. Schmidli, J. Jordan, J. J. Tordoir, M. G. Mohaupt, F. C. Luft, H. Haller, J. Menne and S. Engeli. "Novel baroreflex activation therapy in resistant hypertension: Results of a european multi-center feasibility study." *Journal of the American College of Cardiology* 56 (2010): 1254-58.
69. Shen, M. J. and D. P. Zipes. "Interventional and device-based autonomic modulation in heart failure." *Heart Failure Clinics* 11 (2015): 337-48.
70. La Rovere, M. T. and G. D. Pinna. "Beneficial effects of physical activity on baroreflex control in the elderly." *Annals of Noninvasive Electrocardiology* 19 (2014): 303-10.
71. Laitinen, T., J. Hartikainen, E. Vanninen, L. Niskanen, G. Geelen and E. Länsimies. "Age and gender dependency of baroreflex sensitivity in healthy subjects." *Journal of Applied Physiology* 84 (1998): 576-83.
72. De Meersman, R. E. and P. K. Stein. "Vagal modulation and aging." *Biological psychology* 74 (2007): 165-73.
73. Sandset, E. C., X. Wang, C. Carcel, S. Sato, C. Delcourt, H. Arima, C. Stapf, T. Robinson, P. Lavados and J. Chalmers. "Sex differences in treatment, radiological features and outcome after intracerebral haemorrhage: Pooled analysis of intensive blood pressure reduction in acute cerebral haemorrhage trials 1 and 2." *European stroke journal* 5 (2020): 345-50.
74. Sykora, M., J. Diedler, P. Turcani, W. Hacke and T. Steiner. "Baroreflex: A new therapeutic target in human stroke?" *Stroke* 40 (2009): e678-e82.
75. Nahman-Averbuch, H., L. Dayan, E. Sprecher, U. Hochberg, S. Brill, D. Yarnitsky and G. Jacob. "Sex differences in the relationships between parasympathetic activity and pain modulation." *Physiology & behavior* 154 (2016): 40-48.
76. Fu, Q. and S. Ogoh. "Sex differences in baroreflex function in health and disease." *The journal of physiological sciences* 69 (2019): 851-59.
77. Mendelsohn, M. E. and R. H. Karas. "Molecular and cellular basis of cardiovascular gender differences." *Science* 308 (2005): 1583-87. 10.1126/science.1112062. <Go to ISI>://WOS:000229827000042.
78. Hesse, C., N. Charkoudian, Z. Liu, M. J. Joyner and J. H. Eisenach. "Baroreflex sensitivity inversely correlates with ambulatory blood pressure in healthy normotensive humans." *Hypertension* 50 (2007): 41-6. 10.1161/HYPERTENSIONAHA.107.090308. <https://www.ncbi.nlm.nih.gov/pubmed/17502489>.
79. Casadei, B., A. Pipilis, F. Sessa, J. Conway and P. Sleight. "Low doses of scopolamine increase cardiac vagal tone in the acute phase of myocardial infarction." *Circulation* 88 (1993): 353-57.
80. Matthews, E. L., K. N. Sebzda and M. M. Wenner. "Altered baroreflex sensitivity in young women with a family history of hypertension." *Journal of neurophysiology* 121 (2019): 1011-17.
81. Kingwell, B., J. Cameron, K. Gillies, G. Jennings and A. Dart. "Arterial compliance may influence baroreflex function in athletes and hypertensives." *American Journal of Physiology-Heart and Circulatory Physiology* 268 (1995): H411-H18.
82. Parmer, R. J., J. H. Cervenka and R. A. Stone. "Baroreflex sensitivity and heredity in essential hypertension." *Circulation* 85 (1992): 497-503.